Supplementary Information for:

Titel page:

Novel Conformation Specific Inhibitors of Activated GTPases reveal Ras-dependency of Patient-Derived Cancer Organoids

Authors:

Svenja Wiechmann[1,2], Pierre Maisonneuve[3], Britta M. Grebbin[4,5,6], Meike Hoffmeister[1,7], Manuel Kaulich[1,8], Hans Clevers[9,10,11], Krishnaraj Rajalingam[12], Igor Kurinov[13], Henner F. Farin[4,5,6], Frank Sicheri[3] and Andreas Ernst[1,2,*]

Affiliations:

[1]Institute of Biochemistry II, Goethe University Frankfurt - Medical Faculty, University Hospital, Frankfurt am Main, Germany.

[2]Fraunhofer Institute for Molecular Biology and Applied Ecology IME, Project Group Translational Medicine and Pharmacology TMP, Theodor-Stern-Kai 7, 60590 Frankfurt am Main, Germany.

[3]Lunenfeld-Tanenbaum Research Institute, Sinai Health System, Toronto, ON M5G 1X5, Canada.

[4]German Cancer Consortium (DKTK), 69120 Heidelberg, Germany.

[5]Georg-Speyer-Haus, Institute for Tumor Biology and Experimental Therapy, 60596 Frankfurt am Main, Germany.

[6]German Cancer Research Center (DKFZ), 69120 Heidelberg, Germany.

[7]Institute of Biochemistry, Brandenburg Medical School (MHB) Theodor Fontane, Neuruppin and Brandenburg an der Havel, Germany.

[8]Frankfurt Cancer Institute, Frankfurt am Main, Germany.

[9]Hubrecht Institute, Royal Netherlands Academy of Arts and Sciences (KNAW) and University Medical Center (UMC) Utrecht, Netherlands.

[10]Cancer Genomics Netherlands, UMC Utrecht, Netherlands.

[11]Center for Molecular Medicine, Department of Genetics, UMC Utrecht, Netherlands.

[12]Molecular Signaling Unit-FZI, Institute of Immunology, University Medical Center Mainz, JGU-Mainz, Germany.

[13]Department of Chemistry and Chemical Biology, Cornell University, NE-CAT, Argonne, IL 60439, USA.

*Corresponding author: Andreas Ernst (a.ernst@em.uni-frankfurt.de)

Supplementary Information

Supplementary Figures 1 - 5

Supplementary Fig. 1

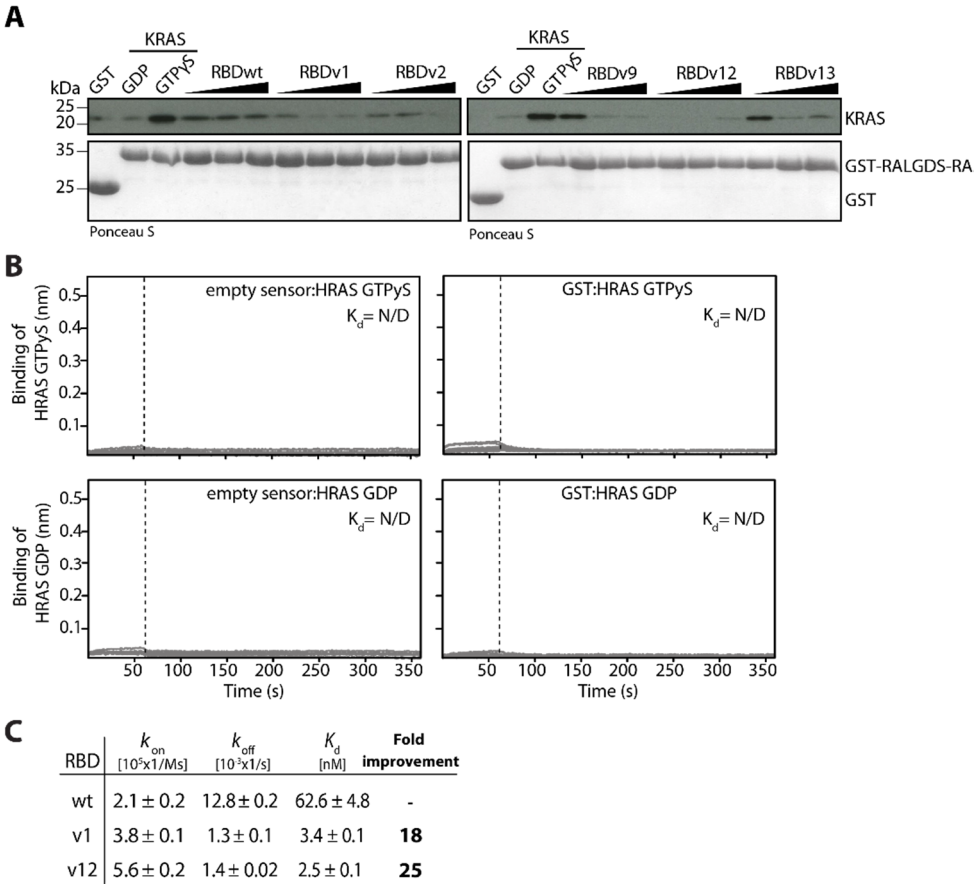

RBD	k_{on} [10^5x1/Ms]	k_{off} [10^{-3}x1/s]	K_d [nM]	Fold improvement
wt	2.1 ± 0.2	12.8 ± 0.2	62.6 ± 4.8	-
v1	3.8 ± 0.1	1.3 ± 0.1	3.4 ± 0.1	**18**
v12	5.6 ± 0.2	1.4 ± 0.02	2.5 ± 0.1	**25**

Supplementary Figure 1 - RBDvs outcompete RalGDS-Ras association domain (RA) binding to activated KRAS.

(**A**) *In vitro* competition of increasing concentration of His-tagged RBDvs and RBDwt and GST-tagged RalGDS-RA immobilized on glutathione sepharose beads binding to His-tagged GTPγS-loaded KRAS. KRAS bound to beads was detected by immunoblot and the corresponding Ponceau S stained membrane is shown.

(**B**) Control experiments of GDP- or GTPγS-loaded HRAS and empty anti-GST biosensors measured by bio-layer interferometry. Concentrations of Ras ranged from 1 µM to 15.6 nM in a 1:1 dilution series. K_d values for could not be calculated due to weak binding. N/D.=not determined.

(**C**) Binding constants for the BLI measurements from Fig. 1D. Values for on rate (k_{on} [10^5x1/Ms]), off rate (k_{off} [10^{-3}x1/s]), dissociation constant (K_d [nM]) and fold improvement are shown.

Supplementary Fig. 2

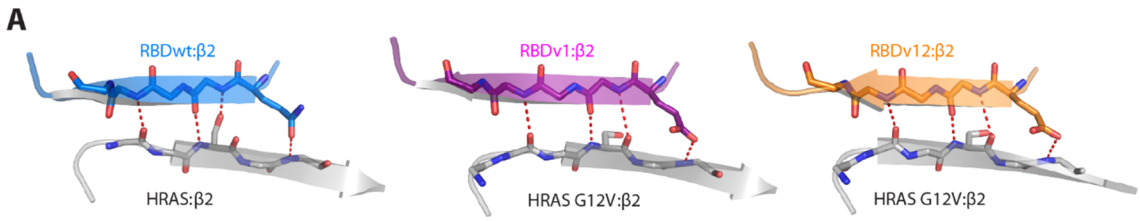

Supplementary Figure 2 - RBDvs bind to HRAS through a canonical binding mode. Detailed view of the canonical extended intermolecular β-sheet at the binding interface of the RBDwt or RBDvs with HRAS or HRAS G12V, respectively. Coloring and labeling are as in Fig. 2A.

Supplementary Fig. 3

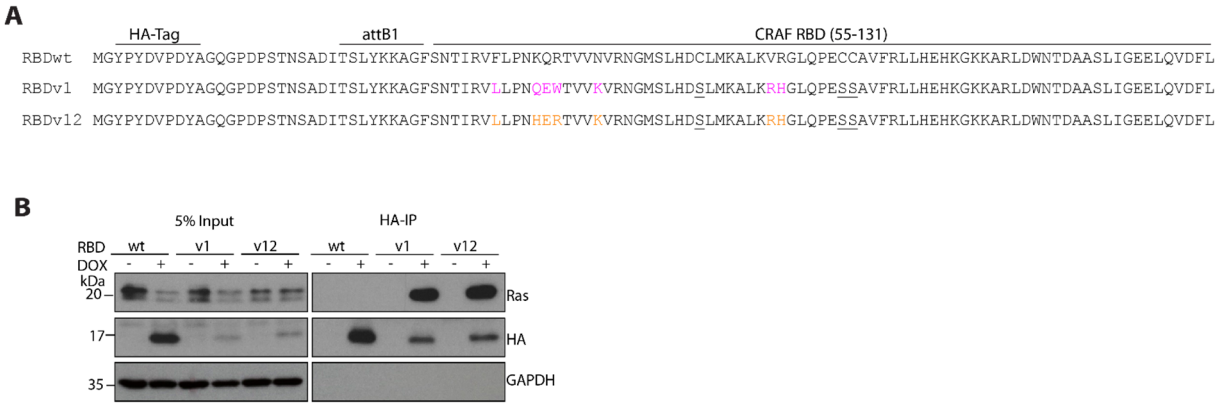

Supplementary Figure 3 - Amino acid sequences of engineered RBDvs and RBDvs are binding to endogenous Ras in HCT 116 cells.

(**A**) Amino acid sequences of HA-tagged RBDwt or RBDvs that were used in this study. Highlighted in bold (magenta and orange in RBDv1 and RBDv12, respectively) are those amino acids that differ from the RBDwt sequence. Underlined are the cysteine to serine mutations in RBDv1 and v12.

(**B**) Western blot of co-immunoprecipitation using anti-HA beads from lentiviral transduced HCT 116 cells stably expressing HA-tagged RBDwt, RBDv1 and RBDv12 upon induction with doxycycline (DOX) (1 µg/ml, 24h) using the indicated antibodies.

Supplementary Fig. 4

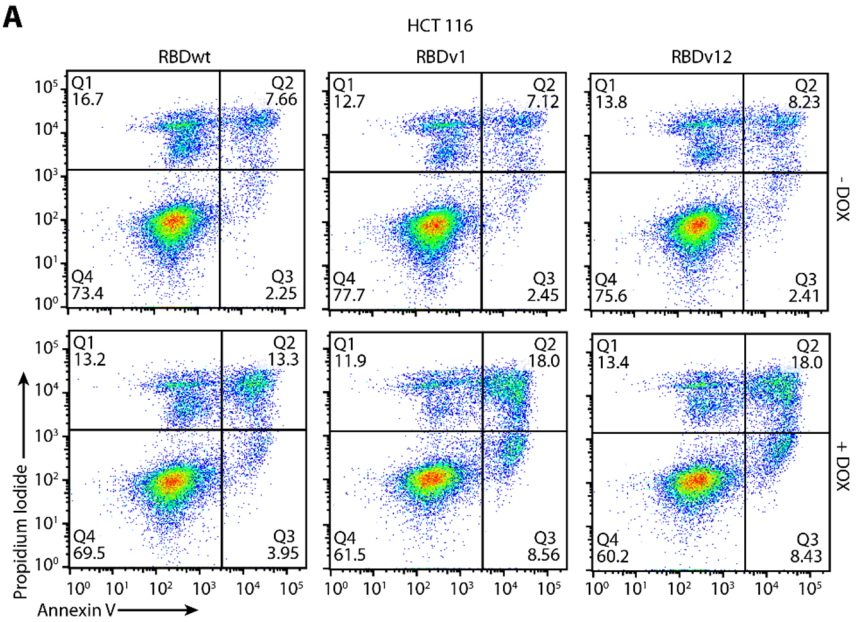

Supplementary Figure 4 - RBDvs induce apoptosis in stable HCT 116 cells. Representative flow cytometry analysis of HCT 116 cells stained with fluorophore labeled annexin V antibody and propidium iodide (PI) by flow cytometry in absence (-DOX) or presence (+DOX) of DOX (1 µg/ml, 72 h).

Supplementary Fig. 5

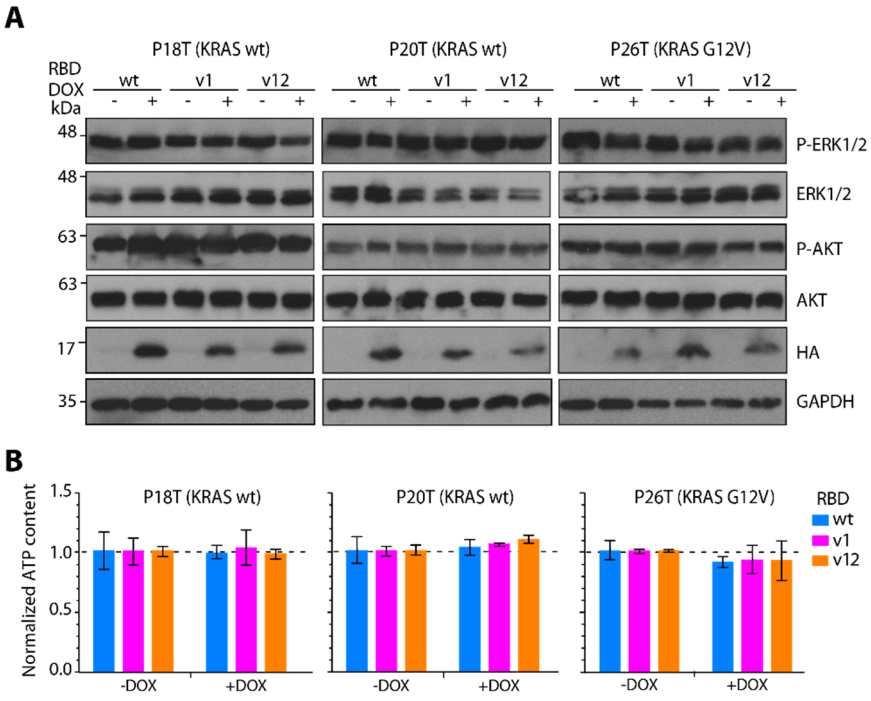

Supplementary Figure 5 - Patient-derived colorectal cancer (CRC) organoids that were insensitive to RBDvs expression.

(**A**) Immunoblot of whole cell lysates derived from indicated patient-derived CRC organoids stably transduced with lentivirus encoding HA-tagged RBDwt, RBDv1 and RBDv12 in absence (-) or presence (+) of DOX (2 µg/ml, 72 h). Cell lysates were analyzed using indicated antibodies.

(**B**) Cellular ATP content of organoid cultures used in (A) expressing RBDwt (blue), RBDv1 (magenta) and RBDv12 (orange) was measured in a luciferase mediated bioluminescence assay. Reduction of cellular ATP in presence of RBDvs (+DOX) was monitored after 72 h induction and normalized to the luminescence of non-induced control organoids (-DOX) (2 µg/ml, 72 h). Error bars correspond to ± SD of three technical replicates (n=3).

Supplementary Tables 1 - 3

Supplementary Table 1: X-Ray data collection and refinement statistics.

	HRAS G12V:RBDv1	HRAS G12V:RBDv12
Data collection		
Space group	P 63 2 2	P 63 2 2
Cell dimensions		
a, *b*, *c* (Å)	91.62, 91.62, 151.41	91.76, 91.76, 151.59
α, β, γ (°)	90, 90, 120	90, 90 ,120
Resolution (Å)	151.4 - 2.9 (3.08 - 2.9)	79.47 – 3.1 (3.31 – 3.1)
R_{meas}	0.14 (10.1)	0.15 (5.31)
$CC_{1/2}$	99.9 (42.3)	99.8 (43.9)
$I / \sigma I$	15.1 (0.4)	11.0 (0.44)
Completeness (%)	99.8 (98.7)	97.9 (90.0)
Redundancy	18.0 (18.7)	12.3 (12.6)
Refinement		
Resolution (Å)	2.9	3.1
R_{work} / R_{free}	22.1 / 25.9	23.8 / 26.8
No. atoms		
Protein	1779	1787
Ligand/ion	39	39
Water	8	1
B-factors		
Protein	136.2	145.7
Ligand/ion	112.0	139.0
Water	100.0	109.3
R.m.s. deviations		
Bond lengths (Å)	0.006	0.0086
Bond angles (°)	1.384	1.5068
Ramachandran statistics		
Residue in favoured regions (%)	96	96.1
Residue in allowed regions (%)	4.0	3.5
Residue in disallowed regions (%)	0	0.4

Supplementary Table 2: Dataset from co-immunoprecipitation and mass spectrometry analysis.

See accompanying data set.

104 **Supplementary Table 3: Cell lines used in this study.**

Name	Cell type	ATCC number	Ras mutation	Zygosity
HCT 116	Human colon cancer cells	ATCC (#CCL-247)	KRAS G13D	Heterozygous
MIA PaCa-2	Human pancreas cancer cells	ATCC (#CRL-1420)	KRAS G12C	Homozygous
A549	Human lung cancer cells	ATCC (#CCL-185)	KRAS G12S	Homozygous
H1299	Human lung cancer cells, derived from metastatic lymph node	ATCC (#CRL-5803)	NRAS Q61K	Heterozygous

105

106